AGU PUBLICATIONS

JGR

Journal of Geophysical Research: Atmospheres

RESEARCH ARTICLE
10.1002/2013JD020720

Key Points:
- Winter $ExCl^-$ is a proxy for sea ice concentration and air temperature
- The primary source of NH_4^+ appears to be biomass burning, not marine
- Seasonal patterns of nitrate observed in the atmosphere are preserved in the ice

Supporting Information:
- Readme
- Figures S1–S5

Correspondence to:
D. R. Pasteris,
daniel.pasteris@dri.edu

Citation:
Pasteris, D. R., J. R. McConnell, S. B. Das, A. S. Criscitiello, M. J. Evans, O. J. Maselli, M. Sigl, and L. Layman (2014), Seasonally resolved ice core records from West Antarctica indicate a sea ice source of sea-salt aerosol and a biomass burning source of ammonium, *J. Geophys. Res. Atmos.*, *119*, 9168–9182, doi:10.1002/2013JD020720.

Received 13 AUG 2013
Accepted 23 JUN 2014
Accepted article online 30 JUN 2014
Published online 21 JUL 2014

Seasonally resolved ice core records from West Antarctica indicate a sea ice source of sea-salt aerosol and a biomass burning source of ammonium

Daniel R. Pasteris[1], Joseph R. McConnell[1], Sarah B. Das[2], Alison S. Criscitiello[3,2], Matthew J. Evans[4], Olivia J. Maselli[1], Michael Sigl[1], and Lawrence Layman[1]

[1]Division of Hydrologic Sciences, Desert Research Institute, Reno, Nevada, USA, [2]Deptartment of Geology and Geophysics, Woods Hole Oceanographic Institution, Woods Hole, Massachusetts, USA, [3]MIT/WHOI Joint Program in Oceanography/Applied Ocean Sciences and Engineering, Woods Hole Oceanographic Institution, Woods Hole, Massachusetts, USA, [4]Department of Chemistry, Wheaton College, Norton, Massachusetts, USA

Abstract The sources and transport pathways of aerosol species in Antarctica remain uncertain, partly due to limited seasonally resolved data from the harsh environment. Here, we examine the seasonal cycles of major ions in three high-accumulation West Antarctic ice cores for new information regarding the origin of aerosol species. A new method for continuous acidity measurement in ice cores is exploited to provide a comprehensive, charge-balance approach to assessing the major non-sea-salt (nss) species. The average nss-anion composition is 41% sulfate (SO_4^{2-}), 36% nitrate (NO_3^-), 15% excess-chloride ($ExCl^-$), and 8% methanesulfonic acid (MSA). Approximately 2% of the acid-anion content is neutralized by ammonium (NH_4^+), and the remainder is balanced by the acidity ($Acy \approx H^+ - HCO_3^-$). The annual cycle of NO_3^- shows a primary peak in summer and a secondary peak in late winter/spring that are consistent with previous air and snow studies in Antarctica. The origin of these peaks remains uncertain, however, and is an area of active research. A high correlation between NH_4^+ and black carbon (BC) suggests that a major source of NH_4^+ is midlatitude biomass burning rather than marine biomass decay, as previously assumed. The annual peak in excess chloride ($ExCl^-$) coincides with the late-winter maximum in sea ice extent. Wintertime $ExCl^-$ is correlated with offshore sea ice concentrations and inversely correlated with temperature from nearby Byrd station. These observations suggest that the winter peak in $ExCl^-$ is an expression of fractionated sea-salt aerosol and that sea ice is therefore a major source of sea-salt aerosol in the region.

1. Introduction

Much of the research on long-term trends in atmospheric aerosol content in Antarctica has come from snow pit and ice core measurements near coastal research stations [*Weller et al.*, 2011; *Wolff et al.*, 2008] or high-elevation deep drilling sites [*De Angelis et al.*, 1987; *Jourdain et al.*, 2008; *Weller and Wagenbach*, 2007]. While these records are important for detailed studies that are difficult in remote locations and for long-term paleoclimate reconstructions, they generally are unable to provide subannually resolved records that are also outside of the local influence of the marine boundary layer.

Subannually resolved ice core records are valuable because they provide an added means by which to assess the source, transport, and deposition mechanisms that affect ice core chemistry. Specifically, the seasonal timing of peaks, troughs, and inflections in the concentration throughout the year provide valuable source and transport information [*Jones et al.*, 2011; *McMorrow et al.*, 2004; *Weller and Wagenbach*, 2007]. The subannual resolution also enables correlation analysis with source tracers during different times of year to assess the possibility of multiple sources.

Present understanding of seasonal aerosol timing in Antarctica includes a maximum of sea-salt aerosols in the winter and a maximum in biogenic sulfur aerosols in the summer [*Jourdain and Legrand*, 2002; *McMorrow et al.*, 2004; *Weller et al.*, 2011]. Ammonium (NH_4^+) previously has been observed to co-occur with biogenic sulfur in the summertime [*Legrand et al.*, 1998; *Savoie et al.*, 1992], and nitrate (NO_3^-) has shown a late-winter/spring peak and a stronger summer peak [*Curran et al.*, 1998; *Jones et al.*, 2011; *Mulvaney et al.*, 1998; *Wagenbach et al.*, 1998b]. This biseasonal pattern in NO_3^- has been interpreted to be from sedimentation of

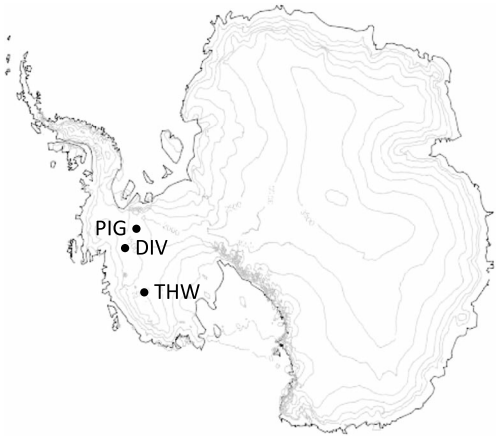

Figure 1. Ice core site locations.

polar stratospheric clouds (PSCs) and snowpack remission during late winter/spring and summer, respectively [*Jones et al*., 2011; *Savarino et al*., 2007; *Wagenbach et al*., 1998b; *Weller et al*., 2002]; however, debate still exists regarding the origin of the summertime peak in high-accumulation coastal locations and the relative magnitude of tropospheric versus stratospheric sources [*Frey et al*., 2009; *Lee et al*., 2014]. The chloride to sodium ratio (Cl^-/Na^+) of aerosols at coastal Antarctic sites has shown a minimum in summer attributed to displacement of volatile chlorine (primarily hydrochloric acid, HCl) from sea-salt aerosols and a maximum in winter that is interpreted as fractionation from mirabilite ($Na_2SO_4{\cdot}10H_2O$) mineral precipitation in sea ice brine prior to aerosol formation [*Hara et al*., 2004, 2012, 2013; *Jourdain and Legrand*, 2002]. Studies of sea-salt aerosols at high-elevation inland sites also have found evidence of fractionation attributed to mirabilite precipitation that peaks in late winter [*Hara et al*., 2004; *Jourdain et al*., 2008].

In this paper we utilize monthly resolved measurements to examine the seasonal characteristics of the acidity and major non-sea-salt ions of three ice cores from West Antarctica. Particular focus is given to NO_3^-, NH_4^+, and excess chloride ($ExCl^-$) since their sources remain uncertain.

2. Methods

Three ice cores were drilled in the summer of 2010/2011 in a moderate elevation, near-coastal region of the West Antarctic ice sheet (WAIS) [*Criscitiello et al*., 2014; *Medley et al*., 2013]. The core locations and other statistics are provided in Figure 1 and Table 1.

The cores were cut into ~1.0 × 0.035 × 0.035 m longitudinal samples at the National Ice Core Laboratory (NICL) in Denver, CO, and transported to the Desert Research Institute (DRI) in Reno, NV, for analysis conducted in October 2011on a continuous melter system. Analysis of Na, Cl, S, Ca, Mg, and Ce was performed continuously by inductively coupled plasma–mass spectrometry (ICP-MS) in a 1% acid matrix. The concentrations of these abundant, soluble elements are assumed to equal their dissolved ionic concentrations because of the very low mineral dust concentration in the ice. The total sulfur measurement (total S) is assumed to equal the sum of sulfate (SO_4^{2-}) and methanesulfonate (MS^-), the latter being the acid anion of methanesulfonic acid (MSA). Measurements of major ions, including MSA, Na^+, and Cl^-, were conducted on replicate longitudinal samples for the years after 1979 by ion chromatography (IC) at Wheaton College in Norton, MA [*Criscitiello et al*., 2013, 2014]. The IC measurements confirm the accuracy of the ICP-MS Na and Cl measurements, and the monthly MSA data have been subtracted from the total S to obtain SO_4^{2-} concentrations after 1979.

Acidity ($Acy = H^+ - HCO_3^-$) was measured continuously on the DRI continuous flow analysis (CFA) system by the recently developed method of *Pasteris et al*. [2012], while NO_3^- and NH_4^+ were measured using traditional CFA methods [*Kaufmann et al*., 2008; *Röthlisberger et al*., 2000]. Black carbon (BC) was measured continuously by laser induced incandescence on a single particle soot photometer (SP2) [*Bisiaux et al*., 2012; *McConnell et al*., 2007].

Table 1. Site Locations and Other Metadata

Core	Latitude (Deg.)	Longitude (Deg.)	Surface Elevation (m)	Core Bottom Depth (m)	Avg. Accum. ($kg\,m^{-2}\,y^{-1}$)
DIV2010	−76.9525	−101.7375	1329	111.8	371
PIG2010	−77.9569	−95.9617	1593	59.5	401
THW2010	−76.7703	−121.2203	2020	61.8	273

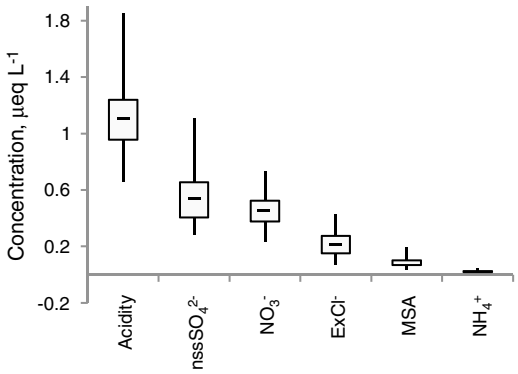

Figure 2. Five-number distributions of average annual concentrations of the non-sea-salt chemical species. Data are from the DIV2010, PIG2010, and THW2010 cores over the period 1979–2010.

Determining the acidity value ($Acy = H^+ - HCO_3^-$) is of greater interest and utility than a simple H^+ measurement because it represents the net acid contribution from species other than carbon dioxide, and the known HCO_3^- (from dissolved CO_2) allows for a charge balance verification to be performed. The HCO_3^- concentration is controlled in the acidity measurement by bubbling the sample with a known partial pressure CO_2 prior to measuring H^+ with a pH probe [*Pasteris et al.*, 2012]. At the average ice core acidity of 1.1 $\mu eq\,L^{-1}$ in this study and an atmospheric partial pressure (Pco_2) of 390 ppm, the H^+ concentration is 3.1 $\mu eq\,L^{-1}$ (pH = 5.493) and the HCO_3^- concentration is 2.0 $\mu eq\,L^{-1}$; therefore, approximately two thirds of the H^+ is derived from CO_2, but this effect is removed by subtracting the known HCO_3^- concentration.

Measurements performed on separate instruments are coregistered in experiment time to an accuracy of ±2 s (1σ) which equates to a depth of 0.003 m ice core depth for this analysis. The error in depth coregistration of the depth-registered signal is slightly more than this because of the asymmetry of sample dispersion combined with differing amounts of dispersion in parallel legs of the CFA system [*Breton et al.*, 2012]. The impact of this error is minimized in our application in three ways, as follows: by coregistering the dispersed time series of electrical conductivity from the different legs of the system, by binning in ice core time intervals of 1 month (~5 cm in the DIV2010 core and 3.5 cm in the THW2010 core), and by averaging multiple months of data to assesses the seasonal timing of the various species discussed in this paper. Assuming normally distributed error caused by dispersion asymmetry, the data coregistration error in the multiyear ($n \geq 10$) monthly averages presented in Figures 4 and 5 is estimated to be less than ±0.5 months (3σ).

Dating of the ice cores was accomplished by identifying the midsummer maximum in three parameters (nssS/Na, H_2O_2, and $\delta^{18}O$) and counting annual cycles. Volcanic time markers present in 1810, 1816, 1885, 1964, and 1992 were used to verify the annual layer counting. Because of the high-accumulation rate and multiple dating parameters, the standard error in the dating is less than ±1 year. Subannual dating was done by linear interpolation between the midsummer annual picks and is estimated to be ±2 months, following the estimates of others in the high-accumulation West Antarctic region [*Abram et al.*, 2011; *Criscitiello et al.*, 2014]. Errors in the subannual dating that arise from random variations in the distribution of snowfall are minimal in the multiyear average annual cycles. The average annual distribution of snowfall is estimated to be uniform because there is no systematic asymmetry in the average annual cycle of H_2O_2 (Figure S1), whose atmospheric concentrations follow the annual solar cycle [*Jouzel et al.*, 1987; *Stewart*, 2004].

Correlations were performed with detrended records in addition to the full (trended) records in order to separately examining high- and low-frequency variability. The detrending was performed by first-order differencing, where $Z_t = X_t - X_{t-1}$. The significance levels of all correlations (p values) were determined by a two-tailed t test where the sample size, N, was adjusted to an effective sample size, N_{ef}, by the method of *Bretherton et al.* [1999] to account for any autocorrelations within the time series [e.g., *Markle et al.*, 2012; *Vance et al.*, 2013]. Considering the detrended correlations in conjunction with the full series correlations shows whether two time series are similar in their low-frequency patterns, their high-frequency patterns, or both. This distinction can be useful for interpreting ice core records that are affected by source and transport processes that vary, in the case of this study, on time scales from seasonal to century scale.

3. Results

A box plot of the distribution of acidity and non-sea-salt acid and base species that affect the acidity is presented in Figure 2. These statistics come from all three ice cores over the period 1979–2010. The most

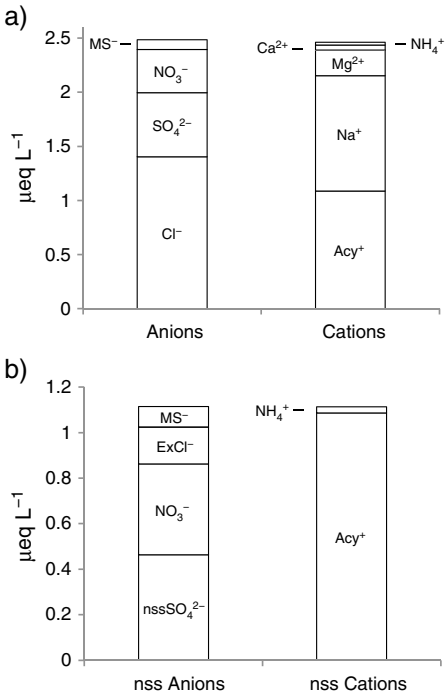

Figure 3. Average concentrations of the major cations and anions in the DIV2010 core over the representative 1984–1998 period. Figure 3a shows all major species, and Figure 3b shows the non-sea-salt species. Measured species with average concentrations greater than 0.02 µeq L^{-1} are shown.

abundant of the acid-anion species in the ice cores is non-sea-salt sulfate ($nssSO_4^{2-}$), which has an average annual value of 0.54 µeq L^{-1} ($\sigma = 0.19$). The next most abundant acid anion is NO_3^- with an average value of 0.45 µeq L^{-1} ($\sigma = 0.11$), followed by excess chloride ($ExCl^-$) with an average value of 0.22 µeq L^{-1} ($\sigma = 0.10$), and then MSA with an average of 0.09 µeq L^{-1} ($\sigma = 0.03$). The non-sea-salt base-cation concentrations are very low, the most abundant of which is NH_4^+ with an average value of 0.020 µeq L^{-1} ($\sigma = 0.007$). Non-sea-salt calcium ($nssCa^{2+}$) and $nssMg^{2+}$ have average annual values less than 0.01 µeq L^{-1} when calculated using bulk seawater ratios. The annual acidity concentration in the three ice cores follows a level trend with an average of 1.12 µeq L^{-1} ($\sigma = 0.25$) over the duration of the records.

The charge balance equation used to verify the acidity measurement and to verify that all major ion species have been identified is the following, with units of µeq L^{-1}:

$$[Acy_{calc}] = [H^+] - [HCO_3^-] = [Cl^-] + [SO_4^{2-}] + [NO_3^-] + [MS^-] - [Na^+] - [Mg^{2+}] - [Ca^{2+}] - [NH_4^+] \quad (1)$$

The average values for these species during a representative time period (1984–1999) in the DIV2010 core are plotted in Figure 3a. The time series of measured acidity and acidity calculated by equation (1) (Acy_{calc}) over this time period are shown in Figure S2. The data in Figure 3, Figure 4, and Figure S2 demonstrate that the sum of the anions and cations are very nearly equal, which indicates that all of the major ions have been included and accurately measured.

An alternate charge balance equation, equation (2), can be derived by removing the charge-neutral sea-salt fraction. This procedure allows for better interpretation of the remaining aerosol sources such as marine phytoplankton, ice sheet boundary layer chemistry, and midlatitude biomass burning or dust events.

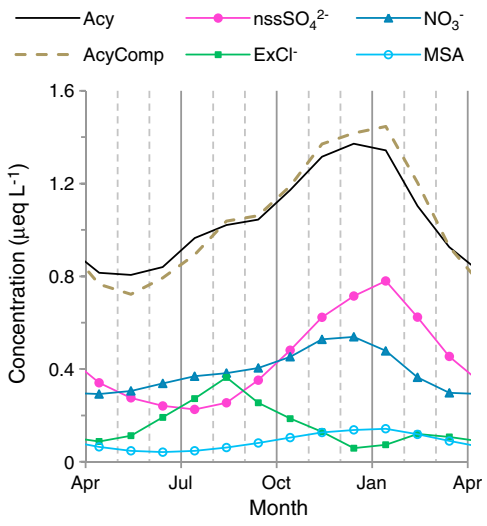

Figure 4. Annual cycles of acidity and the primary acid anions in the DIV2010 ice core. Data points are average monthly concentrations from 1984 to 1999.

$$[Acy_{calc}] = [nssSO_4^{2-}] + [MS^-] + [NO_3^-] + [ExCl^-] - [NH_4^+] - [nssCa^{2+}] - [nssMg^{2+}] \quad (2)$$

$ExCl^-$ is defined as chloride in excess of that expected from the Na^+ concentration and the Cl^-/Na^+ ratio of bulk seawater (molar ratio = 1.167, mass ratio = 1.8) and can hold positive or negative values. Non-sea-salt Ca^{2+} and $nssMg^{2+}$ were determined by the same technique, using the appropriate ratio to sodium concentration in bulk seawater.

It is assumed in equation (2) that all Na^+ is derived from sea-salt aerosol, since mineral dust concentrations in Antarctic ice cores are very low (<2%) during the Holocene at the heavily marine influenced sites in this study [*Röthlisberger et al.*, 2002b]. Another important assumption is that the sea-salt aerosols arriving at the ice core site have the same composition as bulk seawater, i.e., that they have not been fractionated

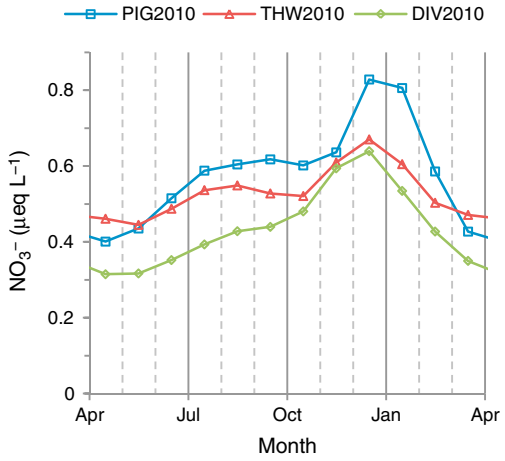

Figure 5. The average annual cycle of NO_3^- at all three sites from 1992 to 2010. The near-surface firn provides the highest subannual sampling resolution due to the lower firn density.

during formation or transport. Although sea-salt aerosols can be fractionated in the cold Antarctic environment [*Rankin et al.*, 2002], we assume bulk seawater composition at this stage of the interpretation and assess the evidence for fractionation in the $ExCl^-$ section, below.

The average non-sea-salt species concentrations in the DIV2010 core from 1984 to 1999 are plotted in Figure 3b, and the time series of these species from 1984 to 1999 are shown in Figure S2. The data show that $nssSO_4^{2-}$ and NO_3^- are present in similar concentrations of 0.46 ($\sigma = 0.27$, $n = 168$ monthly data points) and 0.40 ($\sigma = 0.13$) μeq L^{-1}, respectively. The next most abundant species is $ExCl^-$ with an average concentration of 0.16 ($\sigma = 0.21$) μeq L^{-1} followed by MS^-, the acid anion of MSA, at 0.09 ($\sigma = 0.07$) μeq L^{-1}.

The nss cations (Figure 3b) are composed almost entirely of acidity (net positive $H^+ - HCO_3^-$), with a concentration of 1.1 ($\sigma = 0.41$) μeq L^{-1}, followed by a small amount of NH_4^+ at 0.027 ($\sigma = 0.013$) μeq L^{-1}. The $nssMg^{2+}$ and $nssCa^{2+}$ have average values less than 0.01 μeq L^{-1} and cannot be distinguished from zero within the accuracy of the measurement. The absolute error in the $nssMg^{2+}$ determination is ±0.02 based on the magnitude of the Na^+ and Mg^{2+} concentrations in these ice cores and assuming an accuracy of ±5% in those measurements. Using the same assumptions, the average error in the $ExCl^-$ determination is ±0.06 μeq L^{-1}.

Figure 4 shows the average monthly concentrations, or average annual cycle, of the non-sea-salt acid species during the representative 1984–1999 time period in the DIV2010 core, with time series data from this period shown in Figure S2. The data show that the acidity signal peaks in summer, coinciding with the peak in the sum of the acid anions SO_4^{2-}, NO_3^-, and MSA. The NO_3^- exhibits a pre-maximum shoulder of elevated concentration during late winter (July–Sept., Figure 5) and the $ExCl^-$ exhibits its peak at approximately the same time. These late-winter features in NO_3^- and $ExCl^-$ cause an increase in the acidity at that time, which takes the shape of a pre-maximum shoulder in the annual cycle. The close agreement between the measured and modeled acidity confirms the accuracy and seasonal timing of the major ion species measurements, including the winter peak in $ExCl^-$ that is discussed further below.

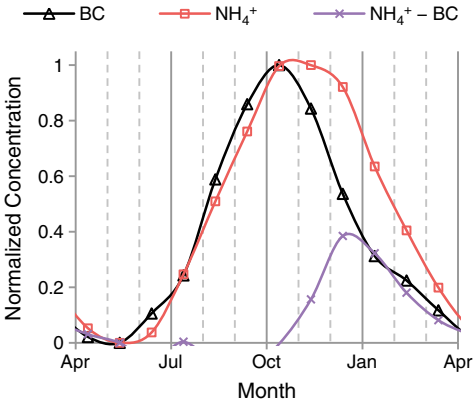

Figure 6. Normalized average annual cycles of the BC and NH_4^+ in the DIV2010 core from 1930 to 1960. NO_3^- is shown for years above the 75th percentile in accumulation ($n = 55$). Also shown is the difference between the normalized NH_4^+ and BC signals. The average concentrations of these species during their respective time sampling periods are 0.17 ppb, 0.024 μeq L^{-1}, and 0.37 μeq L^{-1} for BC, NH_4^+, and NO_3^-, respectively.

Average monthly NH_4^+ concentrations in the DIV2010 core show a broad spring peak from October to December (Figure 6). This timing is very similar to the BC signal, except that the NH_4^+ peak extends further into the summer. As shown in Figure 6, the difference between the two normalized seasonal signals ($NH_4^+ - BC$) peaks in summer and may be the result of a secondary peak in NH_4^+ during summer. This pattern is found in the average annual cycle from all three ice cores, with examples from the THW2010 and PIG2010 cores provided in Figure S3.

4. Discussion

4.1. Nitrate

The annual cycle of NO_3^- shows a primary peak in early summer and a shoulder in late winter, indicating the

presence of two overlapping peaks of unequal strength that may be derived from two separate source or transport processes. The average annual cycle at each site from the well-resolved, low-density firn from 1992 to 2010 is shown in Figure 5. The depth of these samples did not exceed 15 m. Figure S4 shows essentially the same pattern at each site in the well-resolved, high-accumulation years of any age. A similar pattern in NO_3^- concentration, with a primary peak in summer and a secondary peak in late winter, has been observed in freshly fallen snow samples from coastal sites at Halley station and Neumayer station [*Mulvaney et al*., 1998; *Wagenbach et al*., 1998b], and from firn and ice core records from Law Dome [*Curran et al*., 1998; *McMorrow et al*., 2004]. Moderate and low snow accumulation sites including those on the East Antarctic Plateau (EAP) do not preserve the annual cycle well because NO_3^- is reemitted to the atmosphere before it is buried by subsequent snowfall [*Goktas et al*., 2002; *Röthlisberger et al*., 2002a]. The annual cycle of nitrate in this study is also similar to that observed in boundary layer air studies at Neumayer, Mawson, Halley, and Dumont d'Urville, and Kohnen Stations [*Wagenbach et al*., 1998b; *Weller and Wagenbach*, 2007], although at Neumayer and Mawson the timing of the primary atmospheric peak occurs in November and an additional secondary peak in the fall is typically observed [*Wagenbach et al*., 1998b].

The primary source of nitrate in Antarctica is uncertain, but anthropogenic and local marine sources are not likely because the has been no increase in concentration corresponding to recent anthropogenic activity [*Wolff*, 2013] and no elevated nitrate concentrations observed at marine sites or with transport from marine air masses [*Weller et al*., 2002]. Remaining possibilities include the long range transport of natural midlatitude sources through the upper troposphere primarily as NO_x, NO_3^-, or peroxyacetyl nitrate (PAN) [*Lee et al*., 2014], and the incursion of stratospheric sources through air mass exchange or subsidence of polar stratospheric cloud (PSC) particles [*Savarino et al*., 2007; *Wagenbach et al*., 1998b; *Weller et al*., 2002]. Either of these proposed sources could explain the secondary spring peak observed in the present study, since PSC sedimentation and tropospheric sources are expected to produce maximum nitrate concentrations in early spring [*Lee et al*., 2014; *Wagenbach et al*., 1998b].

The timing of the primary peak in NO_3^- during summer found in this and other studies is puzzling because there is no evidence for a maximum in the delivery of primary sources from the troposphere or the stratosphere at this time. However, reemission of nitrate by photolysis to NO_x and evaporation of HNO_3 can provide a local source in the Antarctic boundary layer [*Grannas et al*., 2007; *Röthlisberger et al*., 2002a] which has significant implications for the oxidizing capacity of the Antarctic boundary layer [*Davis et al*., 2004; *Frey et al*., 2013]. This reemission can potentially lead to higher concentrations of nitrate in the surface snow during summer, either through concentration of locally emitted NO_3^- in a "skin layer" at the snow surface [*Erbland et al*., 2013; *Frey et al*., 2009] or possibly emission and advection of reemitted nitrate to downwind locations [*Savarino et al*., 2007]. The concentration of nitrate in ice cores covering a range of accumulation rates from the Dronning Maud Land sector of the EAP has been shown to vary linearly and inversely with surface layer residence time, indicating that substantial export of nitrate away from low accumulation sites can occur [*Pasteris et al*., 2014]. It is unclear whether the primary early summer peak observed in West Antarctica in this study is derived from up-wind emission and advection, local redistribution that forms a transient skin layer, or whether there is an under-recognized primary source mechanism during summer such as the photoxidation of reservoir organic species including PAN or alkyl nitrates [*Jones et al*., 2011; *Lee et al*., 2014; *Munger et al*., 1999]. While uncovering the origin of the primary early summer and secondary late-winter nitrate peaks observed in West Antarctica and elsewhere in Antarctica remains beyond the scope of this study, the many years of seasonally resolved samples archived in West Antarctic ice cores may prove useful for solving the outstanding mysteries of southern high-latitude nitrogen cycling.

4.2. Ammonium

The origin of the NH_4^+ in the ice was investigated further by comparing the long-term record of NH_4^+ with that of the midlatitude biomass burning tracer, black carbon (BC), and the midlatitude dust tracer, cerium (Ce). Cerium is the preferred dust tracer in this study because ~90% of the Ca signal is derived from sea salt, making estimation of the non-sea-salt fraction uncertain. Bulk seawater concentrations [*Turekian*, 1976] indicate that only 0.001% of the Ce signal in this study is derived from seawater, so it is a more direct and reliable dust proxy. Ce is also a useful dust tracer in ice cores [*Simanek*, 2012] because it is the most abundant rare earth element (REE) in the earth's crust, is more easily measured on an ICP-MS, and is a less common contaminant than iron and aluminum.

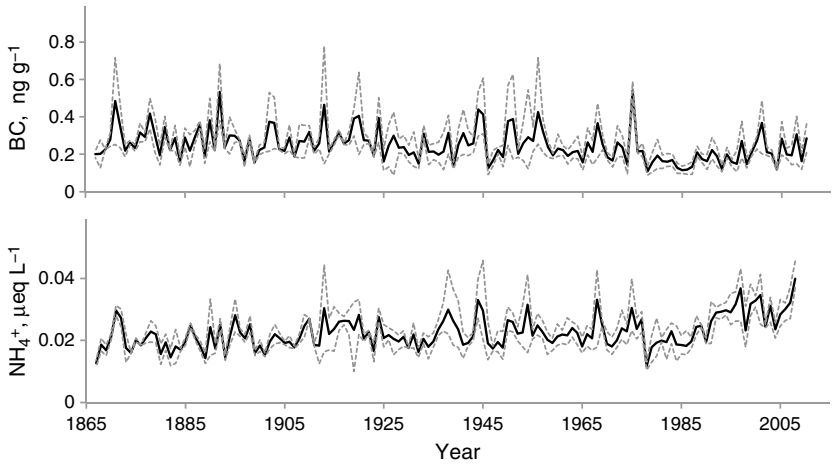

Figure 7. Composite, annually resolved records of BC and NH_4^+ from the three ice cores. The composite (black line) was formed by normalizing and averaging the records together. The maximum and minimum values for each year are shown as the dashed line. The average includes two records (DIV2010 and THW2010) since 1867 and all three records since 1917.

The annually resolved NH_4^+ time series are well correlated at the three sites in this study, and so have been combined into a composite NH_4^+ record to emphasize the features of the signal that are shared within the study region (Figure 7). The same has been done for the BC signal (Figure 7). The combined signals are less prone to anomalies that may arise in a single record due to random variability in precipitation timing, wind, and other factors that affect the preservation of the atmospheric signal in the ice sheet; sampling errors related to missing ice or broken core segments; and analytical errors in the laboratory analysis. Following ice core studies of other chemical species [*Abram et al.*, 2011; *Röthlisberger et al.*, 2010], correlations between BC and NH_4^+ are performed on the log-transformed time series because the annual values are approximately log-normally distributed; thus, the log transformation gives more even consideration to high and low values in the correlation analysis.

The comparison of the annual BC and NH_4^+ records shows that the two species have different long-term trends but very similar interannual variability. The full time series are correlated at $r = 0.39$ ($p < 0.0001$), but after detrending to remove the difference in long-term trend, the NH_4^+ and BC records are remarkably similar and are correlated at $r = 0.73$ ($p << 0.0001$) over the 143 year composite record covering the period 1868–2010. The full and detrended composite BC and NH_4^+ records are overlaid for direct comparison in Figure S5. The same pattern of differing long-term trends, with an increasing ratio of NH_4^+ to BC through time, but very similar interannual variability is found in each of the three individual ice cores. The annual BC and NH_4^+ in the full (trended) records from DIV2010, THW2010, and PIG2010 cores are correlated with r values of 0.42, 0.33, and 0.57, respectively (all $p < 0.0001$), over the full length of each record, while the detrended BC and NH_4^+ are correlated at $r = 0.65$, 0.65, and 0.77, respectively (all $p << 0.0001$). No other elements measured in this study have detrended records correlated so highly with each other, and the next highest detrended correlations are approximately $r = 0.40$. The correlation between composite Ce and BC is $r = 0.23$ for the full time series, and $r = 0.39$ after detrending. The same pattern of correlation between Ce and BC is observed at the individual sites. Since Ce (dust) and BC (biomass burning) in ice-covered Antarctica are known to be derived from separate sources in the midlatitudes, the increased correlations after detrending are interpreted to indicate shared transport from midlatitude regions. Shared transport is probably also a factor in the high-frequency similarity between BC and NH_4^+.

The similarity in interannual variability and the similar seasonal timing of the peak concentration (Figure 6 and Figure S3) between BC and NH_4^+ suggest that they are at least transported together from the midlatitudes, where the biomass burning tracer BC must originate. Since NH_4^+ is also a product of biomass burning and serves as a biomass burning tracer in Greenland ice cores [*Legrand et al.*, 1992], the similarity with the BC signal suggests that NH_4^+ is largely derived from biomass burning in the Antarctic as well. Given the close relationship with BC, it is unlikely that decaying marine biomass in the southern ocean is the dominant source of NH_4^+, as suggested by others [e.g., *Kaufmann et al.*, 2010; *Legrand et al.*, 1998, 1999;

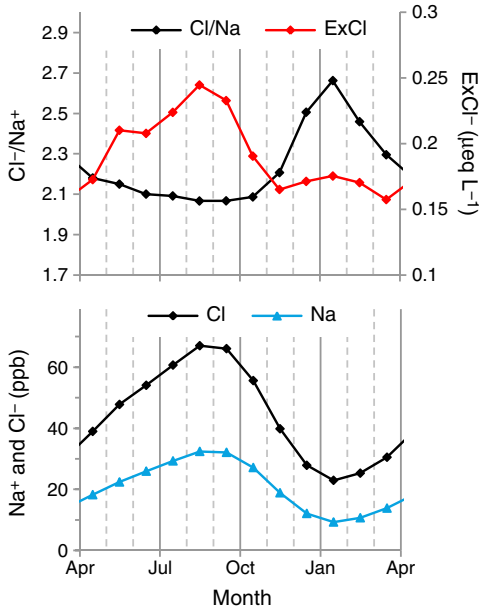

Figure 8. The average annual cycle of $ExCl^-$, Cl^-/Na^+, Na^+, and Cl^- in the THW2010 core from 1967 to 2005.

Wolff, 2012], although it is possible that the ocean could be a secondary source of NH_4^+. A secondary marine source could be the explanation for the apparent summertime secondary peak in NH_4^+ observed in Figure 6 and Figure S3.

It is unclear whether the increasing ratio of NH_4^+ to BC over the period of record is due to changing trends in possible secondary sources of NH_4^+ or BC, such as coal burning (BC), fertilizer use (NH_4^+), or marine biomass decay (NH_4^+). It is possible that anthropogenic influences have led to a change in biomass burning patterns that could have led to a change in the NH_4^+ to BC ratio. Given the apparent primary midlatitude source of NH_4^+ in Antarctica, further study focused on the relationship between NH_4^+ and BC may lead to a better understanding of long-term changes in their midlatitude sources, including biomass burning, biogenic production, and fossil fuel burning.

4.3. Excess Chloride and the Cl^-/Na^+ Ratio

The annual cycle of $ExCl^-$ shows monthly concentrations that are positive year round with a maximum in late winter (Figure 4). The charge balance assessment with the acidity measurement serves to verify the magnitude and timing of the $ExCl^-$ annual cycle. Positive values of $ExCl^-$ can arise from the deposition of volatile chloride (mostly HCl) from the lower troposphere that has been displaced from sea-salt aerosols by sulfuric and nitric acids, MSA, or N_2O_5 [*Erickson et al.*, 1999; *Hara et al.*, 2005; *Yao and Zhang*, 2012; *Zhao and Gao*, 2008]; however, this chloride displacement process is less extensive during winter than in summer in Antarctica [*Hara et al.*, 2005; *Hara et al.*, 2013; *Jourdain and Legrand*, 2002] and is not expected to provide enough chloride for generation of a winter peak in the $ExCl^-$ signal. Excess chloride can also occur if the sea-salt aerosol is depleted in Na^+ (increased Cl^-/Na^+ratio) due to mirabilite mineral precipitation ($Na_2SO_4{\cdot}10H_2O$) from a salt water brine at the sea ice-air interface [*Rankin et al.*, 2002; *Wolff et al.*, 2003]. The fractionated brine can be transferred to frost flowers and the snow surface by wicking and blown into the air by the wind to form fractionated sea-salt aerosols that are deposited to the ice sheet. The sea ice source for aerosol with depleted Na^+ only occurs in winter, because the salt water brine above the sea ice must reach temperatures below −8°C for mirabilite precipitation to occur [*Marion et al.*, 1999]. Fractionated sea-salt aerosol particles depleted in SO_4^{2-} [*Abram et al.*, 2013 and references therein; *Wagenbach et al.*, 1998a] and Na^+ [*Hara et al.*, 2012, 2013] have been observed to be abundant during Antarctic winter and attributed to mirabilite precipitation and a sea ice source. The prevalence of the sea ice source of sea-salt aerosol versus the open ocean source remains the subject of ongoing research, however [e.g. *Abram et al.*, 2013; *Hara et al.*, 2012; *Jourdain et al.*, 2008; *Spolaor et al.*, 2013; *Wolff et al.*, 2003], and whether the potential sea ice source is dominated by windblown frost flowers or blowing snow is also uncertain [*Abram et al.*, 2013; *Yang et al.*, 2008].

The question of whether fractionated sea-salt aerosol is responsible for the winter $ExCl^-$ concentration can be investigated using winter season $ExCl^-$ and Cl^-/Na^+ values from the ice cores. Unfortunately, a contaminated baseline in the chloride measurement that stemmed from analyzing acidified samples with an HCl matrix in the laboratory prior to the ice core analysis has affected the accuracy of the long-term trend of the chloride measurement in DIV and PIG cores and in the THW core prior to 1967 (depth > 22.7 m). The upper 22.7 m of the THW core was analyzed at a later time and experienced no problems with the chloride measurement and are considered fully accurate within the typical range of ±5%. While the baseline issue in question affects the long-term trend in the chloride measurement and $ExCl^-$ time series, the relative interannual variability is not significantly affected, so the detrended records from DIV2010 and PIG2010 can be used in support of the findings from the full and detrended record from the THW2010 core.

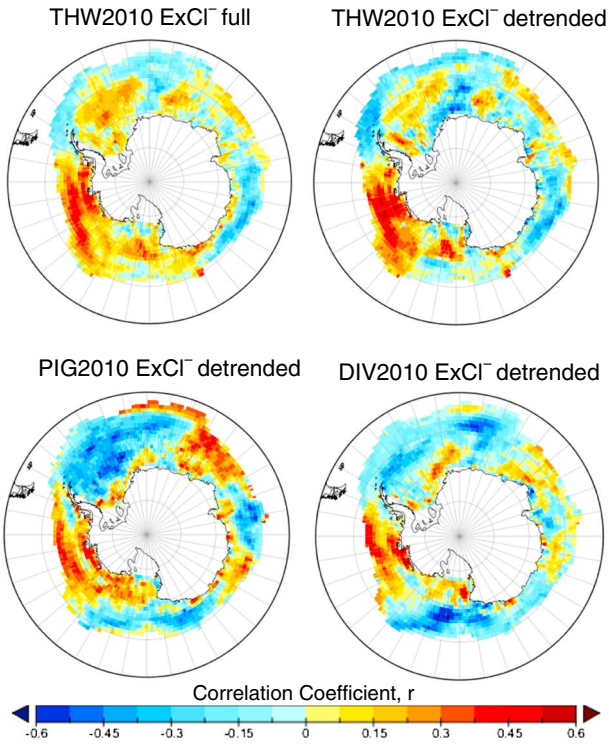

Figure 9. Correlation maps of winter (June to September (JJAS)) $ExCl^-$ with average winter (June to October (JJASO)) sea ice concentration from the HadISST data set [*Rayner et al.*, 2003]. The correlations with $ExCl^-$ in the PIG2010 and DIV2010 cores are detrended due to analytical uncertainty in the long-term trend of the chloride measurement. The correlation coefficient with p value less than 10% is 0.33, less than 5% is 0.37, less than 1% is 0.48, and <0.1% ($p < 0.001$) is 0.57. Outliers were removed in 1997 at THW, 1998 at PIG, and 2004 at DIV in order to better capture the overall correlation pattern.

The annual cycles of $ExCl^-$ and Cl^-/Na^+ for the THW2010 core from 1967 to 2005 are shown in Figure 8 and match the findings from DIV2010 presented in Figure 4 and Figure S2. The late-winter (June to September (JJAS)) peak in $ExCl^-$ corresponds to the time of greatest sea-salt aerosol concentration as indicated by the Na^+ and Cl^- annual cycles (Figure 8). The data show that that $ExCl^-$ is present in small amounts during summer and that Cl^-/Na^+ is generally higher in summer than in winter, but $ExCl^-$ is lower in summer because overall sea-salt concentrations are lower at that time of year. The summertime $ExCl^-$ chloride may be derived from volatile chloride that is displaced from sea-salt aerosols in the atmosphere during summer. This process has been observed to be more extensive during summer than winter due to the presence of acids and higher temperatures [*Hara et al.*, 2013; *Jourdain and Legrand*, 2002], so volatile chloride is not expected to contribute significantly to $ExCl^-$ during winter. It is not expected that significant amounts of chloride would mix between summer and winter layers via diffusion or wind pumping in the snowpack given the high snow accumulation rates. Average layer thickness in the THW core is 65 cm in the top 5 m, 85 cm at DIV, and 95 cm at PIG.

In the following analysis, wintertime (JJAS) $ExCl^-$ values have been correlated with average wintertime sea ice concentration (SIC) data from the HadISST data set [*Rayner et al.*, 2003]. In addition, average wintertime Cl^-/Na^+ was correlated with net sea ice formation (SIF), e.g., $SIC_{Sept} - SIC_{May}$, and with winter temperatures from an instrumental record available from nearby Byrd station [*Bromwich et al.*, 2013]. The $ExCl^-$ concentrations are influenced by the Cl^-/Na^+ ratio of the sample and the total concentration of sea-salt aerosol (see Results for $ExCl^-$ definition); thus, $ExCl^-$ is positively correlated with Na^+ concentration and the Cl^-/Na^+ ratio. The winter Cl^-/Na^+ ratio is not correlated with total sea-salt aerosol concentration, however, indicating that the bulk Cl^-/Na^+ ratio is not a function of total sea-salt aerosol load.

The winter time (JJAS) $ExCl^-$ in the ice cores is well correlated to winter sea ice concentration (June to October (JJASO)) in the Bellingshausen-Amundsen Sea (Figure 9). Detrended records are used from the DIV2010 and PIG2010 sites due to the analytical problem with the long-term trend of Cl^-. The full record (with trend) from the THW2010 is well correlated with the sea ice, and the detrended record is presented as well, for direct comparison. All three sites show similar twin bands of high correlation: one in the near coastal zone of Bellingshausen-Amundsen sea and the other farther out near the line of maximum sea ice extent. The near-shore band may impact the $ExCl^-$ because of its proximity to the ice core sites, and the maximum extent band may signify that total ice area is important, but further investigation will be necessary to understand this pattern. Evidence is visible of the dipole structures in SIC that have been previously observed [*Yuan and Martinson*, 2000], where SIC in the Pacific sector varies opposite to that in the Atlantic sector, and similar to that of the Indian Ocean sector [*Landrum et al.*, 2012]. Consistent with the findings of *Criscitiello et al.* [2013], who used total Cl^-, the $ExCl^-$ at the DIV2010 site is well correlated with SIC within the area of Pine Island Bay and Amundsen Sea polynyas, indicating that sea-salt aerosol

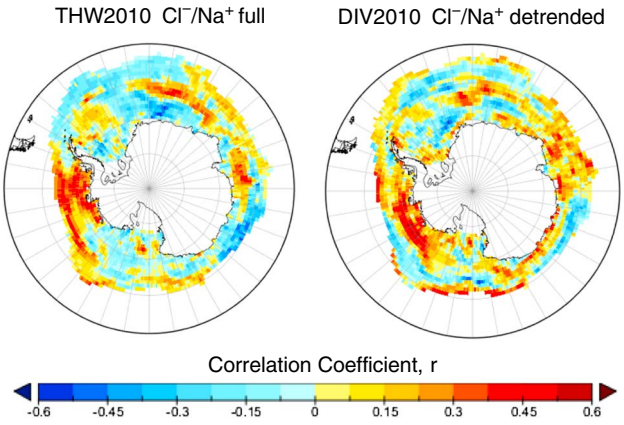

Figure 10. Correlation map of winter Cl^-/Na^+ with sea ice formation (SIF) from May through September. June ice formation ($SIC_{Jun} - SIC_{May}$) is weighted twice in the total, so $SIF = 2 \times (SIC_{Jun} - SIC_{May}) + 1 \times (SIC_{Sep} - SIC_{Jun})$. Outlier years 1997 and 2004 were removed from the THW2010 and DIV2010 analysis, respectively.

concentration may be derived from the ice-covered polynyas and could be used as a proxy for polynya opening [*Criscitiello et al.*, 2013].

The Cl^-/Na^+ ratio, which varies independent of total sea-salt concentration, is also correlated with sea ice formation in the Bellingshausen-Amundsen sea at the THW2010 and DIV2010 sites (Figure 10). A statistically significant increase in the correlation (a greater adjusted-R^2) is found when counting June ice formation ($SIC_{Jun} - SIC_{May}$) twice in the total, so $SIF = 2 \times (SIC_{Jun} - SIC_{May}) + 1 \times (SIC_{Sep} - SIC_{Jun})$. Although significant sea ice formation occurs in the months of April and May [*Landrum et al.*, 2012], SIF prior to June is not positively correlated with the Cl^-/Na^+ ratio in the ice cores. This lack of correlation holds true when April and May are included in the wintertime ice core Cl^-/Na^+ average, rather than limiting the time frame to the JJAS time period. These observations of positive correlation between Cl^-/Na^+ and SIF during mid to late winter, when air temperatures are coldest are consistent with the occurrence of fractionated sea-salt aerosol by mirabilite precipitation [*Alvarez-Aviles et al.*, 2008; *Douglas et al.*, 2012; *Rankin et al.*, 2002].

The possible influence of cold temperature processes on wintertime $ExCl^-$ is further supported by inverse correlations of winter (JJAS) Cl^-/Na^+ and Mg^{2+}/Na^+ in the THW2010 core with winter temperatures (JJAS) from nearby Byrd station (Figure 11). Mg^{2+} is the next most abundant sea-salt component after Cl^- and Na^+, so it is also a sea-salt tracer that should be relatively free of influence from secondary dust sources [*Hara et al.*, 2012]. Thus, an increase in the bulk Mg^{2+}/Na^+ ratio should also occur when there is Na^+ depletion due to mirabilite precipitation as has been observed in aerosol particle studies [*Hara et al.*, 2012]. From the beginning of the high quality Cl^- data in 1967, and with the removal of one outlier in 2000, the Cl^-/Na^+ record is inversely correlated at $r = -0.48$ ($p < 0.001$) and $r = -0.72$ ($p < 0.0001$) after detrending. The Mg^{2+}/Na^+, after removal of one outlier in 1977, is inversely correlated at $r = -0.40$ ($p < 0.01$) and $r = -0.57$ ($p < 0.001$) after detrending. The outliers are depicted in the time series plots in Figure 11, and removal of one from each series of 44 years is considered reasonable given the possibility of subannual dating inaccuracy, secondary sources, or other random sampling or analytical error. Besides $ExCl^-$ and $ExMg^{2+}$, which are less well correlated,

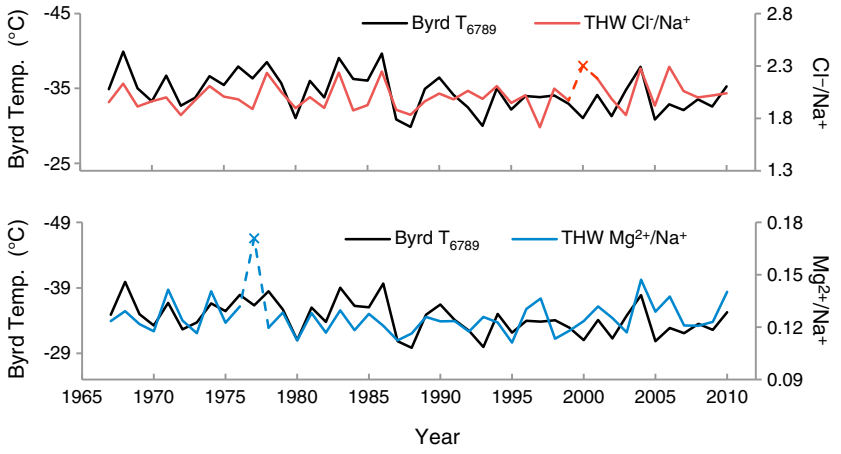

Figure 11. Time series of winter (JJAS) ice core Cl^-/Na^+ and Mg^{2+}/Na^+ with winter (JJAS) temperature from Byrd Station.

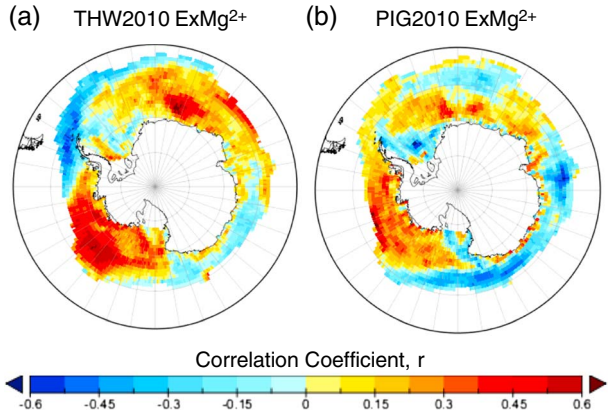

Figure 12. Correlation of winter (JJAS) excess magnesium ($ExMg^{2+}$) with average winter sea ice concentration (JJASO) for the (a) THW2010 and (b) PIG2010 ice cores. The correlations are with the full (trended) time series from 1979 to 2010. No outliers were removed from the THW analysis, and 2010 was removed from the PIG analysis.

the Cl^-/Na^+ and Mg^{2+}/Na^+ ratios are the only aerosol species or species ratios that are significantly correlated with the Byrd temperature record. A final piece of evidence that sea ice and mirabilite precipitation are responsible for the winter Cl^- and Mg^{2+} excesses and enrichments in the ice cores is that, similar to $ExCl^-$, $ExMg^{2+}$ is also correlated to sea ice concentration (JJASO) in the Bellingshausen-Amundsen Sea (Figure 12). The correlation maps in Figure 12 show a broad area of $ExMg^{2+}$ correlation with sea ice concentration in the Amundsen Sea and Southern Ocean.

A comprehensive investigation of the mechanisms affecting winter $ExCl^-$ is beyond the scope of this study and deserves further research; however, the preliminary findings presented here are in line with existing knowledge and observations of a fractionated sea-salt aerosol source. We cannot rule out that the observed correlations could be caused by a separate process besides sea ice formation that is also related to temperature, such as aerosol transport or post-depositional effects; however, no evidence or established mechanism can be found in the literature to support such a process. Among alternatives to consider include whether low winter temperatures are consistently associated with low snow accumulation leading to subannual winter ice core samples that contain more snow from spring and fall than during warm years. This could explain why cold years are associated with higher Cl^-/Na^+ ratios, which peak in summer (Figure 8), but would not explain higher $ExCl^-$ values which peak in winter. It also would not explain why no other species or species ratios are significantly correlated with Byrd temperature, including those that have summer peaks such as H_2O_2 and $nssS/Na^+$. A secondary source of volatile chloride is expected to be present in summer, but its transfer and preservation in winter layers as a function of temperature seem unlikely, especially given the thick annual layers of over 65 cm at the surface. Nitrate is a volatile summertime component of snowpack chemistry and shows no such relation to the Byrd temperature record. A substantial secondary source of Cl^- or Mg^+ during winter also appears unlikely since the Cl^-/Na^+ and Mg^{2+}/Na^+ ratios are not inversely correlated with Na^+ concentration as is the case for other ratios to Na^+ that are clearly derived from separate sources, such as BC/Na^+, Ce/Na^+, NO_3^-/Na^+, or $nssS/Na^+$.

Low winter temperatures could also be associated with changes in aerosol transport to the ice core sites. Previous studies indicate that low pressure centers over the Bellingshausen-Amundsen Sea are associated with cold temperatures and sea ice formation in the region [*Bromwich et al.*, 2013; *Criscitiello et al.*, 2014; *Landrum et al.*, 2012]. The wind associated with the low pressure systems would presumably aid in the generation and transport of sea-salt aerosols from either an open ocean or a sea ice source, however, and does not affect the argument that the $ExCl^-$ and Cl^-/Na^+ could be a reflection of sea ice fractionation processes. Transport variability may affect the degree to which the fractionated aerosol signature appears in the ice cores though and should be considered in addition to the cold temperature sea ice source in future investigations.

It is also possible that a wintertime process of volatile chloride displacement from sea-salt aerosols or surface snow may be affecting the winter $ExCl^-$ and Cl^-/Na^+ ratios. Although chloride volatilization is expected to be minor during winter, more research devoted to its generation on sea-salt aerosols and in near-surface snow will be useful in determining its impact. Reasons behind the differences between the correlation pattern between $ExMg^{2+}$ and $ExCl^-$ also remain unclear, but secondary sources of $ExCl^-$ and $ExMg^{2+}$ such as volatile chloride and mineral dust, combined with subannual winter sampling error, could be responsible. Another outstanding question is why the winter Cl^-/Na^+ ratios occasionally rise to values of 2.5, when the theoretical upper limit from mirabilite fractionation is 2.05 (Figure 11). It is not clear whether this a winter time sampling issue, evidence of a secondary source of volatile chloride, or incomplete understanding of the fractionation

process. In sum, while the correlations of Cl^- and Mg^{2+} ratios and excesses with sea ice concentration and temperature are consistent with a sea-salt fractionation process, more detailed study is necessary to confirm the abundance of fractionated sea-salt aerosols in the snow pack and to better rule out the influence of secondary sources.

An additional outcome of these results, if the winter $ExCl^-$ peak is indeed derived from fractionated sea-salt aerosols, would be a change in the assessment of the non-sea-salt charge balance in Figure 3b and Figure 4. The wintertime $ExCl^-$ as computed using bulk seawater ratios would instead belong to a charge-balanced sea-salt aerosol that would be missing equal parts Na^+ and SO_4^{2-} (in μeq units) due to mirabilite precipitation. The result would be an increase in $nssSO_4^{2-}$ during the June–September time period that would give the annual cycle in $nssSO_4^{2-}$ a late-winter shoulder similar to that found in the NO_3^- annual cycle. Such an effect is not visible in the nssS data; however, the effects of sea-salt fractionation on sulfur concentrations in bulk samples are difficult to observe due to the presence of biogenic sulfur [*Hara et al*., 2012; *Jourdain et al*., 2008], which may itself be affected by sea ice conditions [*Criscitiello et al*., 2013; *Curran et al*., 2003].

5. Summary and Conclusions

The acidity and major ions have been characterized in three West Antarctic ice cores dating back to the 1780s. The non-sea-salt anions that affect the acidity are $nssSO_4^{2-}$, NO_3^-, $ExCl^-$, and MS^-, with average concentrations of 0.54, 0.45, 0.22, and 0.09 μeq L^{-1}, respectively. The non-sea-salt cations are comprised almost entirely of Acy ($H^+ - HCO_3^-$) plus a small amount of NH_4^+, which have average concentrations of 1.12 and 0.02 μeq L^{-1}, respectively. Organic acid anions besides MS^- were not measured but are expected to have an average concentration of ≤0.02 μeq L^{-1} [*Legrand and Saigne*, 1988].

The average annual cycles of the major ions share features with those found in atmospheric aerosol studies in Antarctica. The NO_3^- annual cycle shows a primary peak in early summer (~Nov–Jan) and a secondary peak in later-winter/spring (~Aug–Sept.). The annual cycle of NO_3^- is consistent with previous studies that attribute the secondary late-winter/spring peak to sedimentation of polar stratospheric cloud particles and the primary summer peak to snowpack reemissions of reactive nitrogen (NO_y); however, these hypotheses remain tentative. The subannual nitrate signal is well resolved within the top ~15 m of the snowpack at the sites it this study, which contain ~20 years of data and are easily accessible by hand auger or mechanical drill. It may be possible to gain new insights into the sources of NO_3^- in Antarctica using ice cores from the WAIS by analyzing the isotope composition of NO_3^-, stratospheric tracers such as ^{10}Be and ^{210}Pb, or other analytes from the many years of seasonally resolved samples, similar to what has been done in bulk aerosol studies [e.g., *Wagenbach et al*., 1998b].

The annual cycle of NH_4^+ shows a primary spring peak that coincides with the annual peak in BC and is very highly correlated with BC, providing strong evidence that the primary source of NH_4^+ in this region is biomass burning. The normalized annual cycle of NH_4^+ shows a secondary peak in summer that is not present in the BC signal, indicating a secondary source that could be the marine source observed in previous coastal studies [*Legrand et al*., 1998]. In light of the evidence for a predominant biomass burning source of NH_4^+ in this study, care should be taken when interpreting NH_4^+ from non-coastal locations in Antarctica as a proxy for marine biomass decay. An observed decrease in the BC/NH_4^+ ratio during the 20th century may indicate a change in secondary sources of BC and NH_4^+, including a possible decrease in anthropogenic BC during the first half of the 20th century.

The annual cycle of $ExCl^-$ exhibits a maximum in late winter that is consistent with the timing of increased sea ice concentration around Antarctica. Winter season $ExCl^-$ is well correlated with winter sea ice concentration in the Bellingshausen-Amundsen sea at all three ice core sites, suggesting that sea ice could be the source of the sea-salt aerosols and the $ExCl^-$ values. $ExMg^{2+}$ is also correlated with sea ice concentration at the THW and DIV sites, consistent with the excess values being caused from Na^+ depletion by mirabilite precipitation on the sea ice surface. The Cl^-/Na^+ and Mg^{2+}/Na^+ ratios at the THW site are inversely correlated with instrumental temperature at the nearby Byrd site, further implicating sea ice as the source of the sea-salt aerosols, since Na^+ depletion by mirabilite precipitation can only occur when sea ice brine temperatures are below −8°C. We cannot rule out that other processes related to cold temperatures and/or sea ice formation

could be responsible for the observed Cl^- and Mg^{2+} ratios and excesses, but no such processes that could affect both Cl^- and Mg^{2+} in this way have been identified. Future research into sea-salt ratios in ice cores and volatile chloride cycling will be helpful in verifying whether sea ice is the source of the wintertime sea-salt aerosols and whether sea-salt fractionation is the source of the wintertime $ExCl^-$.

Acknowledgments
The data used to produce the figures in this paper can be obtained by contacting the authors. This work was supported by grants from the NSF Antarctic Program (0632031 and 1142166), NSF-MRI (1126217), the NASA Cryosphere Program (NNX10AP09G), and by an award from the Department of Energy Office of Science Graduate Fellowship Program (DOE SCGF) to ASC. The authors would like to thank the field crews who collected the samples and students who assisted with the laboratory analysis.

References

Abram, N. J., R. Mulvaney, and C. Arrowsmith (2011), Environmental signals in a highly resolved ice core from James Ross Island, Antarctica, *J. Geophys. Res.*, *116*, D20116, doi:10.1029/2011JD016147.

Abram, N. J., E. W. Wolff, and M. A. J. Curran (2013), A review of sea ice proxy information from polar ice cores, *Quat. Sci. Rev.*, *79*(0), 168–183, doi:10.1016/j.quascirev.2013.01.011.

Alvarez-Aviles, L., W. R. Simpson, T. A. Douglas, M. Sturm, D. Perovich, and F. Domine (2008), Frost flower chemical composition during growth and its implications for aerosol production and bromine activation, *J. Geophys. Res.*, *113*, D21304, doi:10.1029/2008JD010277.

Bisiaux, M. M., R. Edwards, J. R. McConnell, M. A. J. Curran, T. D. Van Ommen, A. M. Smith, T. A. Neumann, D. R. Pasteris, J. E. Penner, and K. Taylor (2012), Changes in black carbon deposition to Antarctica from two high-resolution ice core records, 1850–2000 AD, *Atmos. Chem. Phys.*, *12*(9), 4107–4115, doi:10.5194/acp-12-4107-2012.

Bretherton, C. S., M. Widmann, V. P. Dymnikov, J. M. Wallace, and I. Blade (1999), The effective number of spatial degrees of freedom of a time-varying field, *J. Clim.*, *12*(7), 1990–2009, doi:10.1175/1520-0442(1999)012<1990:tenosd>2.0.co;2.

Breton, D. J., B. G. Koffman, A. V. Kurbatov, K. J. Kreutz, and G. S. Hamilton (2012), Quantifying signal dispersion in a Hybrid Ice Core Melting System, *Environ. Sci. Technol.*, *46*(21), 11,922–11,928, doi:10.1021/es302041k.

Bromwich, D. H., J. P. Nicolas, A. J. Monaghan, M. A. Lazzara, L. M. Keller, G. A. Weidner, and A. B. Wilson (2013), Central West Antarctica among the most rapidly warming regions on Earth, *Nat. Geosci.*, *6*(2), 139–145, doi:10.1038/ngeo1671.

Criscitiello, A. S., S. B. Das, M. J. Evans, K. E. Frey, H. Conway, I. Joughin, B. Medley, and E. J. Steig (2013), Ice sheet record of recent sea-ice behavior and polynya variability in the Amundsen Sea, West Antarctica, *J. Geophys. Res. Oceans*, *118*, 118–130, doi:10.1029/2012JC008077.

Criscitiello, A. S., S. B. Das, K. B. Karnauskas, M. J. Evans, K. E. Frey, I. Joughin, E. J. Steig, J. R. McConnell, and B. Medley (2014), Tropical Pacific influence on the source and transport of marine aerosols to West Antarctica, *J. Clim.*, *27*(3), 1343–1363, doi:10.1175/jcli-d-13-00148.1.

Curran, M. A. J., T. D. van Ommen, and V. Morgan (1998), Seasonal characteristics of the major ions in the high-accumulation Dome Summit South ice core, Law Dome, Antarctica, *Ann. Glaciol.*, *27*, 385–390.

Curran, M. A. J., T. D. van Ommen, V. I. Morgan, K. L. Phillips, and A. S. Palmer (2003), Ice core evidence for Antarctic sea ice decline since the 1950s, *Science*, *302*(5648), 1203–1206, doi:10.1126/science.1087888.

Davis, D., G. Chen, M. Buhr, J. Crawford, D. Lenschow, B. Lefer, R. Shetter, F. Eisele, L. Mauldin, and A. Hogan (2004), South Pole NOx chemistry: An assessment of factors controlling variability and absolute levels, *Atmos. Environ.*, *38*(32), 5375–5388, doi:10.1016/j.atmosenv.2004.04.039.

De Angelis, M., N. I. Barkov, and V. N. Petrov (1987), Aerosol concentrations over the last climatic cycle (160 kyr) from an Antarctic ice core, *Nature*, *325*(6102), 318–321.

Douglas, T. A., et al. (2012), Frost flowers growing in the Arctic ocean–atmosphere-sea ice-snow interface: 1. Chemical composition, *J. Geophys. Res.*, *117*, D00R09, doi:10.1029/2011JD016460.

Erbland, J., W. C. Vicars, J. Savarino, S. Morin, M. M. Frey, D. Frosini, E. Vince, and J. M. F. Martins (2013), Air-snow transfer of nitrate on the East Antarctic Plateau - Part 1: Isotopic evidence for a photolytically driven dynamic equilibrium in summer, *Atmos. Chem. Phys.*, *13*(13), 6403–6419, doi:10.5194/acp-13-6403-2013.

Erickson, D. J., C. Seuzaret, W. C. Keene, and S. L. Gong (1999), A general circulation model based calculation of HCl and $ClNO_2$ production from sea salt dechlorination: Reactive Chlorine Emissions Inventory, *J. Geophys. Res.*, *104*(D7), 8347–8372, doi:10.1029/98JD01384.

Frey, M. M., J. Savarino, S. Morin, J. Erbland, and J. M. F. Martins (2009), Photolysis imprint in the nitrate stable isotope signal in snow and atmosphere of East Antarctica and implications for reactive nitrogen cycling, *Atmos. Chem. Phys.*, *9*(22), 8681–8696, doi:10.5194/acp-9-8681-2009.

Frey, M. M., N. Brough, J. L. France, P. S. Anderson, O. Traulle, M. D. King, A. E. Jones, E. W. Wolff, and J. Savarino (2013), The diurnal variability of atmospheric nitrogen oxides (NO and NO_2) above the Antarctic Plateau driven by atmospheric stability and snow emissions, *Atmos. Chem. Phys.*, *13*(6), 3045–3062, doi:10.5194/acp-13-3045-2013.

Goktas, F., H. Fischer, H. Oerter, R. Weller, S. Sommer, and H. Miller (2002), A glacio-chemicalcharacterization of the new EPICA deep-drilling site on Amundsenisen, Dronning Maud Land, Antarctica, *Ann. Glaciol.*, *35*(35), 347–354, doi:10.3189/172756402781816474.

Grannas, A. M., et al. (2007), An overview of snow photochemistry: Evidence, mechanisms and impacts, *Atmos. Chem. Phys.*, *7*(16), 4329–4373.

Hara, K., K. Osada, M. Kido, M. Hayashi, K. Matsunaga, Y. Iwasaka, T. Yamanouchi, G. Hashida, and T. Fukatsu (2004), Chemistry of sea-salt particles and inorganic halogen species in Antarctic regions: Compositional differences between coastal and inland stations, *J. Geophys. Res.*, *109*, D20208, doi:10.1029/2004JD004713.

Hara, K., K. Osada, M. Kido, K. Matsunaga, Y. Iwasaka, G. Hashida, and T. Yamanouchi (2005), Variations of constituents of individual sea-salt particles at Syowa station, Antarctica, *Tellus Ser. B Chem. Phys. Meteorol.*, *57*(3), 230–246, doi:10.1111/j.1600-0889.2005.00142.x.

Hara, K., K. Osada, M. Yabuki, and T. Yamanouchi (2012), Seasonal variation of fractionated sea-salt particles on the Antarctic coast, *Geophys. Res. Lett.*, *39*, L18801, doi:10.1029/2012GL052761.

Hara, K., K. Osada, and T. Yamanouchi (2013), Tethered balloon-borne aerosol measurements: Seasonal and vertical variations of aerosol constituents over Syowa Station, Antarctica, *Atmos. Chem. Phys.*, *13*(17), 9119–9139, doi:10.5194/acp-13-9119-2013.

Jones, A. E., et al. (2011), The multi-seasonal NOy budget in coastal Antarctica and its link with surface snow and ice core nitrate: Results from the CHABLIS campaign, *Atmos. Chem. Phys.*, *11*(17), 9271–9285, doi:10.5194/acp-11-9271-2011.

Jourdain, B., and M. Legrand (2002), Year-round records of bulk and size-segregated aerosol composition and HCl and HNO_3 levels in the Dumont d'Urville (coastal Antarctica) atmosphere: Implications for sea-salt aerosol fractionation in the winter and summer, *J. Geophys. Res.*, *107*(D22), 4645 doi:10.1029/2002JD002471.

Jourdain, B., S. Preunkert, O. Cerri, H. Castebrunet, R. Udisti, and M. Legrand (2008), Year-round record of size-segregated aerosol composition in central Antarctica (Concordia station): Implications for the degree of fractionation of sea-salt particles, *J. Geophys. Res.*, *113*, D14308, doi:10.1029/2007JD009584.

Jouzel, J., G. L. Russell, R. J. Suozzo, R. D. Koster, J. W. C. White, and W. S. Broecker (1987), Simulations of the HDO and $H_2{}^{18}O$ atmospheric cycles using the NASA GISS general circulation model: The seasonal cycle for present-day conditions, *J. Geophys. Res.*, *92*(D12), 14,739–14,760, doi:10.1029/JD092iD12p14739.

Kaufmann, P. R., U. Federer, M. A. Hutterli, M. Bigler, S. Schupbach, U. Ruth, J. Schmitt, and T. F. Stocker (2008), An improved continuous flow analysis system for high-resolution field measurements on ice cores, *Environ. Sci. Technol.*, *42*(21), 8044–8050, doi:10.1021/es8007722.

Kaufmann, P. R., et al. (2010), Ammonium and non-sea salt sulfate in the EPICA ice cores as indicator of biological activity in the Southern Ocean, *Quat. Sci. Rev.*, *29*(1–2), 313–323, doi:10.1016/j.quascirev.2009.11.009.

Landrum, L., M. M. Holland, D. P. Schneider, and E. Hunke (2012), Antarctic sea ice climatology, variability, and late twentieth-century change in CCSM4, *J. Clim.*, *25*(14), 4817–4838, doi:10.1175/jcli-d-11-00289.1.

Lee, H.-M., D. K. Henze, B. Alexander, and L. T. Murray (2014), Investigating the sensitivity of surface-level nitrate seasonality in Antarctica to primary sources using a global model, *Atmos. Environ.*, *89*, 757–767, doi:10.1016/j.atmosenv.2014.03.003.

Legrand, M., and C. Saigne (1988), Formate, acetate and methanesulfonate measurements in antarctic ice - some geochemical implications, *Atmos. Environ.*, *22*(5), 1011–1017, doi:10.1016/0004-6981(88)90278-8.

Legrand, M., M. De Angelis, T. Staffelbach, A. Neftel, and B. Stauffer (1992), Large perturbations of ammonium and organic-acids content in the Summit-Greenland Ice Core. Fingerprint from forest fires?, *Geophys. Res. Lett.*, *19*(5), 473–475, doi:10.1029/91GL03121.

Legrand, M., F. Ducroz, D. Wagenbach, R. Mulvaney, and J. Hall (1998), Ammonium in coastal Antarctic aerosol and snow: Role of polar ocean and penguin emissions, *J. Geophys. Res.*, *103*(D9), 11,043–11,056, doi:10.1029/97JD01976.

Legrand, M., E. Wolff, and D. Wagenbach (1999), Antarctic aerosol and snowfall chemistry: Implications for deep Antarctic ice-core chemistry, *Ann. Glaciol.*, *29*, 66–72, doi:10.3189/172756499781821094.

Marion, G. M., R. E. Farren, and A. J. Komrowski (1999), Alternative pathways for seawater freezing, *Cold Reg. Sci. Technol.*, *29*(3), 259–266, doi:10.1016/s0165-232x(99)00033-6.

Markle, B. R., N. A. N. Bertler, K. E. Sinclair, and S. B. Sneed (2012), Synoptic variability in the Ross Sea region Antarctica, as seen from back-trajectory modeling and ice core analysis, *J. Geophys. Res.*, *117*, D02113, doi:10.1029/2011JD016437.

McConnell, J. R., R. Edwards, G. L. Kok, M. G. Flanner, C. S. Zender, E. S. Saltzman, J. R. Banta, D. R. Pasteris, M. M. Carter, and J. D. W. Kahl (2007), 20th-century industrial black carbon emissions altered arctic climate forcing, *Science*, *317*(5843), 1381–1384, doi:10.1126/science.1144856.

McMorrow, A., T. D. Van Ommen, V. Morgan, and M. A. J. Curran (2004), Ultra-high-resolution seasonality of trace-ion species and oxygen isotope ratios in Antarctic firn over four annual cycles, *Ann. Glaciol.*, *39*, 34–40, doi:10.3189/172756404781814609.

Medley, B., et al. (2013), Airborne-radar and ice-core observations of annual snow accumulation over Thwaites Glacier, West Antarctica confirm the spatiotemporal variability of global and regional atmospheric models, *Geophys. Res. Lett.*, *40*, 3649–3654, doi:10.1002/grl.50706.

Mulvaney, R., D. Wagenbach, and E. W. Wolff (1998), Postdepositional change in snowpack nitrate from observation of year-round near-surface snow in coastal Antarctica, *J. Geophys. Res.*, *103*(D9), 11,021–11,031, doi:10.1029/97JD03624.

Munger, J. W., D. J. Jacob, S. M. Fan, A. S. Colman, and J. E. Dibb (1999), Concentrations and snow-atmosphere fluxes of reactive nitrogen at Summit, Greenland, *J. Geophys. Res.*, *104*(D11), 13,721–13,734, doi:10.1029/1999JD900192.

Pasteris, D. R., J. R. McConnell, and R. Edwards (2012), High-resolution, continuous method for measurement of acidity in ice cores, *Environ. Sci. Technol.*, *46*(3), 1659–1666, doi:10.1021/es202668n.

Pasteris, D. R., J. R. McConnell, R. Edwards, E. Isaksson, and M. R. Albert (2014), Acidity decline in Antarctic ice cores during the Little Ice Age linked to changes in atmospheric nitrate and sea salt concentrations, *J. Geophys. Res. Atmos.*, *119*, 5640–5652, doi:10.1002/2013JD020377.

Rankin, A. M., E. W. Wolff, and S. Martin (2002), Frost flowers: Implications for tropospheric chemistry and ice core interpretation, *J. Geophys. Res.*, *107*(D23), 4683 doi:10.1029/2002JD002492.

Rayner, N. A., D. E. Parker, E. B. Horton, C. K. Folland, L. V. Alexander, D. P. Rowell, E. C. Kent, and A. Kaplan (2003), Global analyses of sea surface temperature, sea ice, and night marine air temperature since the late nineteenth century, *J. Geophys. Res.*, *108*(D14), 4407 doi:10.1029/2002JD002670.

Röthlisberger, R., M. Bigler, M. Hutterli, S. Sommer, B. Stauffer, H. G. Junghans, and D. Wagenbach (2000), Technique for continuous high-resolution analysis of trace substances in firn and ice cores, *Environ. Sci. Technol.*, *34*(2), 338–342, doi:10.1021/es9907055.

Röthlisberger, R., et al. (2002a), Nitrate in Greenland and Antarctic ice cores: A detailed description of post-depositional processes, *Ann. Glaciol.*, *35*(35), 209–216, doi:10.3189/172756402781817220.

Röthlisberger, R., R. Mulvaney, E. W. Wolff, M. A. Hutterli, M. Bigler, S. Sommer, and J. Jouzel (2002b), Dust and sea salt variability in central East Antarctica (Dome C) over the last 45 kyrs and its implications for southern high-latitude climate, *Geophys. Res. Lett.*, *29*(20), 1963 doi:10.1029/2002GL015186.

Röthlisberger, R., X. Crosta, N. J. Abram, L. Armand, and E. W. Wolff (2010), Potential and limitations of marine and ice core sea ice proxies: An example from the Indian Ocean sector, *Quat. Sci. Rev.*, *29*(1–2), 296–302, doi:10.1016/j.quascirev.2009.10.005.

Savarino, J., J. Kaiser, S. Morin, D. M. Sigman, and M. H. Thiemens (2007), Nitrogen and oxygen isotopic constraints on the origin of atmospheric nitrate in coastal Antarctica, *Atmos. Chem. Phys.*, *7*(8), 1925–1945.

Savoie, D. L., J. M. Prospero, R. J. Larsen, and E. S. Saltzman (1992), Nitrogen and sulfur species in aerosols at Mawson, Antarctica, and their relationship to natural radionuclides, *J. Atmos. Chem.*, *14*(1–4), 181–204, doi:10.1007/bf00115233.

Simanek, R. (2012), *Cerium in Ice Cores as a Tracer of Mineral Dust*, 106 pp., Univ. of Nevada, Reno.

Spolaor, A., et al. (2013), Halogen species record Antarctic sea ice extent over glacial-interglacial periods, *Atmos. Chem. Phys.*, *13*(13), 6623–6635, doi:10.5194/acp-13-6623-2013.

Stewart, R. W. (2004), The annual cycle of hydrogen peroxide: An indicator of chemical instability?, *Atmos. Chem. Phys.*, *4*, 933–946.

Turekian, K. K. (1976), *Oceans (Foundations of Earth Science Series)*, 149 pp., Prentice Hall College Div., Englewood Cliff, N. J.

Vance, T. R., T. D. van Ommen, M. A. J. Curran, C. T. Plummer, and A. D. Moy (2013), A millennial proxy record of ENSO and Eastern Australian rainfall from the law dome ice core, East Antarctica, *J. Clim.*, *26*(3), 710–725, doi:10.1175/jcli-d-12-00003.1.

Wagenbach, D., F. Ducroz, R. Mulvaney, L. Keck, A. Minikin, M. Legrand, J. S. Hall, and E. W. Wolff (1998a), Sea-salt aerosol in coastal Antarctic regions, *J. Geophys. Res.*, *103*(D9), 10,961–10,974, doi:10.1029/97JD01804.

Wagenbach, D., M. Legrand, H. Fischer, F. Pichlmayer, and E. W. Wolff (1998b), Atmospheric near-surface nitrate at coastal Antarctic sites, *J. Geophys. Res.*, *103*(D9), 11,007–11,020, doi:10.1029/97JD03364.

Weller, R., and D. Wagenbach (2007), Year-round chemical aerosol records in continental Antarctica obtained by automatic samplings, *Tellus Ser. B Chem. Phys. Meteorol.*, *59*(4), 755–765, doi:10.1111/j.1600-0889.2007.00293.x.

Weller, R., A. E. Jones, A. Wille, H. W. Jacobi, H. P. McIntyre, W. T. Sturges, M. Huke, and D. Wagenbach (2002), Seasonality of reactive nitrogen oxides (NOy) at Neumayer Station, Antarctica, *J. Geophys. Res.*, *107*(D23), 4673 doi:10.1029/2002JD002495.

Weller, R., D. Wagenbach, M. Legrand, C. Elsasser, X. Tian-Kunze, and G. Konig-Langlo (2011), Continuous 25-yr aerosol records at coastal Antarctica - I: Inter-annual variability of ionic compounds and links to climate indices, *Tellus Ser. B Chem. Phys. Meteorol.*, *63*(5), 901–919, doi:10.1111/j.1600-0889.2011.00542.x.

Wolff, E. W. (2012), Chemical signals of past climate and environment from polar ice cores and firn air, *Chem. Soc. Rev.*, *41*(19), 6247–6258, doi:10.1039/c2cs35227c.

Wolff, E. W. (2013), Ice sheets and nitrogen, *Philos. Trans. R. Soc. London, Ser. B*, *368*(1621), doi:10.1098/rstb.2013.0127.

Wolff, E. W., A. M. Rankin, and R. Röthlisberger (2003), An ice core indicator of Antarctic sea ice production?, *Geophys. Res. Lett.*, *30*(22), 2158 doi:10.1029/2003GL018454.

Wolff, E. W., A. E. Jones, S. J. B. Bauguitte, and R. A. Salmon (2008), The interpretation of spikes and trends in concentration of nitrate in polar ice cores, based on evidence from snow and atmospheric measurements, *Atmos. Chem. Phys.*, *8*(18), 5627–5634, doi:10.5194/acp-8-5627-2008.

Yang, X., J. A. Pyle, and R. A. Cox (2008), Sea salt aerosol production and bromine release: Role of snow on sea ice, *Geophys. Res. Lett.*, *35*, L16815, doi:10.1029/2008GL034536.

Yao, X. H., and L. M. Zhang (2012), Chemical processes in sea-salt chloride depletion observed at a Canadian rural coastal site, *Atmos. Environ.*, *46*, 189–194, doi:10.1016/j.atmosenv.2011.09.081.

Yuan, X. J., and D. G. Martinson (2000), Antarctic sea ice extent variability and its global connectivity, *J. Clim.*, *13*(10), 1697–1717, doi:10.1175/1520-0442(2000)013<1697:asieva>2.0.co;2.

Zhao, Y. L., and Y. Gao (2008), Acidic species and chloride depletion in coarse aerosol particles in the US east coast, *Sci. Total Environ.*, *407*(1), 541–547, doi:10.1016/j.scitotenv.2008.09.002.